

N88-11167

EXPERIMENTAL DETERMINATION OF FLOW POTENTIAL SURFACES
SUPPORTING A MULTIAXIAL FORMULATION OF VISCOPLASTICITY

J. R. Ellis and D. N. Robinson
The University of Akron
Akron, Ohio

INTRODUCTION

The form and framework of constitutive relationships for structural metals are closely tied to the concepts of a potential function and normality. For example, in elasticity the complementary energy function (or thermodynamically, the related Gibbs free energy) has the properties of a potential and the strain vector can be interpreted geometrically as lying normal to surfaces of constant complementary energy density. The existence of the complementary energy function (or its dual, the strain energy density function) is not just a theoretical contrivance but relates directly to the path independence and reversibility that is the essence of elasticity. In plasticity, the yield function plays the role of a potential and the inelastic strain increment (or rate) vector is directed normal to the yield surface. Analogously, this implies a form of path independence in plasticity, not in the complete sense as in elasticity, but in an incremental sense. In either case, it is the potential/normality structure that provides a consistent framework of a multiaxial theory. The validity of this structure has been experimentally ascertained (refs. 1-6) for a wide class of structural alloys under conditions where their mechanical behavior can be idealized as being largely time-independent, e.g., under relatively low strain rates and at low homologous temperatures.

At high homologous temperature structural metals exhibit inherently time-dependent behavior. Moreover, most important structural applications involve not only high temperature but severe temperature transients and gradients as well. Thus, time (or rate) and temperature are key variables and the development of constitutive equations unavoidably must be guided by and consistent with a general thermodynamic framework.

The thermodynamics of inelastic solids in terms of internal state variables has been discussed by several authors. In some studies (e.g., ref. 7) the internal variables are taken to be phenomenological parameters whose physical origin and associated evolutionary laws are not readily identified. Other studies (refs. 8-12) have attempted to identify internal variables with specific local microstructural rearrangements, e.g., local slip rearrangements on crystallographic planes resulting from dislocation motion and interaction. In these studies the emphasis is on rigorous local representation of rate or growth laws supplemented with an averaging procedure to obtain a macroscopic constitutive law. Consistent with either of these points of view is the assumption and adoption of a flow potential function

$$\Omega = \Omega (\sigma_{ij}, T, \alpha_g) \quad (1)$$

that controls the internal dissipation. Here we consider only small quasistatic

deformations and take Ω as depending on stress σ_{ij} , temperature T and internal variables denoted by α_β ($\beta = 1, 2, \dots, n$). Practical theories to date have incorporated, at most, two state variables, i.e., a tensorial state variable (internal or back stress) and a scalar variable (drag or threshold stress).

The existence of a (convex) flow potential function together with the generalized normality structure:

$$\dot{\epsilon}_{ij} = \frac{\partial \Omega}{\partial \sigma_{ij}} \quad (2)$$

$$-\dot{\alpha}_\beta / h = \frac{\partial \Omega}{\partial \alpha_\beta} \quad (3)$$

where h is a scalar function of the internal state variables and $\dot{\epsilon}_{ij}$ the inelastic strain rate, assures a positive entropy production rate as demanded by the second law of thermodynamics. Further, as discussed in references 13 and 14, this potential/normality structure also assures reasonable continuum properties in structural problems, e.g., uniqueness and important convergence properties. So again, as in the case of the classical theories discussed above, the potential/normality structure is precisely that which provides the framework of a consistent multi-axial theory. Knowledge of the form of Ω and the demonstrated validity of the normality concept allows the forms of the flow law (eq. (2)) and the evolutionary law (eq. (3)) to be specified; this is possible only through appropriate multi-axial testing. This (exploratory) testing should be aimed at revealing the general features of behavior for classes of alloys and not take the form of detailed (characterization) tests furnishing a data base for a specific material in a specific condition. Exploratory experiments, in this sense, provide guidance to the development of a consistent theoretical framework.

Thus it is seen that Ω plays an analogous role to the yield surface in classical plasticity. Examples of postulated forms of Ω are given in references 9, 12, and 15-17. Experimental evidence for the existence of a flow potential function has been found in preliminary studies reported in references 18 and 19 and recently and more comprehensively in reference 20.

As discussed in references 21 and 22, flow potential surfaces are, under conditions of interest, identifiable with surfaces of constant inelastic strain rate (SCISR's). It is the direct experimental measurement of SCISR's, together with an assessment of the concept of normality, that is the subject of the research presented here. The approach is to conduct experiments under biaxial (tension-torsion) states of stress by making use of an extension (refs. 21, 23) of the probing technique used extensively in yield surface probing experiments conducted in support of the classical theory of plasticity (refs. 1-6).

In the following sections we first present the details of the experimental procedure followed in a preliminary set of experiments conducted on the representative alloy type 316 stainless steel. Although primary interest is in the determination of initial and subsequent SCISR's at high homologous temperatures (e.g., ~ 0.5), the preliminary tests were conducted at a lower temperatures (~ 0.2) largely because of

experimental convenience. Nevertheless, significant time-dependent response at the lower temperature allowed SCISR measurements to be carried out and an evaluation of the experimental technique made.

Results of the preliminary tests are presented showing three of a family of initial SCISR's, including strain rate vectors for assessing the condition of normality. Conclusions are drawn concerning the feasibility of the experimental technique, the nature of the measured SCISR's and an assessment of the normality condition. Finally, a discussion is given concerning future research.

EXPERIMENTAL DETAILS

As noted above, the test equipment and procedures used to determine SCISR's are similar to those used in yield surface investigations. The experiments are conducted under computer control on MTS electrohydraulic test systems. The type of specimen used is the thin-walled tube and the type of loading is tension-torsion. This approach produces stress states which are homogeneous and directly calculable from the known external loading. Prior to installation in the test system, specimens are instrumented with four rectangular strain gage rosettes. These strain gages are used to calibrate the high precision, multi-axial extensometer used in the SCISR experiments. This is accomplished by cycling the specimen within its elastic range and adjusting the outputs of the extensometer until they are identical to those of the strain gages. Further, these experiments provide values of elastic modulus (E) and shear modulus (G) which subsequently are used for control purposes. The test setup described above is shown in figure 1.

Test system control in SCISR experiments is accomplished using four independent measurements. These are total axial strain (ϵ) and total shear strain (γ), obtained using the biaxial extensometer, and axial stress (σ) and torsional stress (τ), obtained using a tension-torsion load cell. During individual probes, specimens are loaded radially, $\tau/\sigma = \text{constant}$, at predetermined stress rates. The corresponding elastic strain rates, $\dot{\sigma}/E$ and $\dot{\tau}/G$, are calculated using known values of elastic moduli. During the loading, total axial strain and total shear strain are monitored by the computer. The corresponding values of total strain rate, $\dot{\epsilon}$ and $\dot{\gamma}$, are obtained by making these measurements over predetermined time increments and calculating the rates. Taking total strain rate to be the sum of the elastic and inelastic components, the two inelastic strain rate components are calculated as follows:

$$\dot{\epsilon}_p = \dot{\epsilon} - \dot{\sigma}/E \quad (4)$$

$$\dot{\gamma}_p = \dot{\gamma} - \dot{\tau}/G \quad (5)$$

where $\dot{\epsilon}_p$ is the axial component of inelastic strain rate and $\dot{\gamma}_p$ is the torsional component. Equivalent inelastic strain rate (I) is calculated using the expression

$$I = (\dot{\epsilon}_p^2 + 1/3 \dot{\gamma}_p^2)^{1/2} \quad (6)$$

When I reaches a target value, $100 \mu\epsilon/m$ in the subject experiments, the probe is terminated and the specimen unloaded. The same computer program allows probes to be conducted at 16 preset angles in tension-torsion stress space. The results of these tests subsequently are used to establish the locus of points corresponding to the target value of inelastic strain rate in tension-torsion stress space. The experimental approach outlined above is shown schematically in figure 2.

Regarding the material details, the material tested was type 316 stainless steel, Republic Steel heat 8092297, supplied in solution annealed condition in the form of 64 mm O.D. bar. After manufacture, the specimen was subjected to the following heat-treatment: Heat to 1065°C , hold for 30 minutes, cool at $149^{\circ}\text{C}/\text{min}$ to 537°C , and continue cooling at a convenient rate to room temperature. This heat-treatment was performed in flowing argon to prevent specimen oxidation. An examination of the materials microstructure after the above heat-treatment showed it to be equiaxed with grain size in the range 2-4 ASTM units. A series of micro-hardness measurements made in both longitudinal and transverse senses showed that the material's hardness was reasonably uniform, the DPH values obtained being in the range 120 to 140.

EXPERIMENTAL RESULTS

Several techniques were used to acquire data in these experiments. One approach was to monitor the signals from the load cell and the extensometer directly using X-Y plotters and strip chart recorders. The aim here was to have a visual representation of the data as the test progressed, data in this form being particularly useful in identifying problems as they arose. The data acquisition system (DAS) was also used to check for experimental difficulties. The approach adopted was to calculate the current value of inelastic strain rate as a percentage of the target value and to print this percentage at 1 second intervals. Outputs of this form were useful in identifying "noise" problems. Also, the final values of the stress and strain were printed at the end of each probe along with the axial and torsional components of inelastic strain rate. The SCISR and strain rate vectors shown in figure 3 were constructed using data obtained in this manner.

In addition to controlling the test, the DAS was used to store the measured values of axial stress, axial strain, torsional stress and torsional strain on magnetic tape at 1 second intervals. These data subsequently were used for detailed post-test analysis of the results. As a first step in this analysis, plots of stress versus time, strain versus time, and stress versus strain were prepared for both the axial and torsional components of loading. These data were used to evaluate the performance of the control system and also the performance of the various measurement systems. Data free from experimental difficulties were reduced further as illustrated in figures 4 and 5, using results obtained in Probe (14). The curves shown in figure 4 were determined using equations (4) and (5) while the curve shown in figure 5 was determined using equation (6). As indicated in figure 5, it was possible to use curves of this type to determine SCISR's ranging from threshold to the target value of $100 \mu\epsilon/\text{in}$. The family of SCISR's shown in figure 6 were established in this manner for nine probes judged free from experimental difficulty.

CONCLUSIONS AND DISCUSSION

The following general conclusions have been drawn from the preliminary experimental results:

- The proposed experimental method for directly determining surfaces at constant inelastic strain rate (SCISR's), at a fixed inelastic state, appears feasible. This has been demonstrated, at least, in the neighborhood of the virgin state.
- The members of the family of initial SCISR's shown have the expected general shape, order, and spacing. Experimental scatter appears minimal and a reasonably regular, convex figure is defined. The elliptical figures are not too different from those predicted for a fully isotropic J_2 -type material.
- Although some departure from strict normality of the strain-rate vectors to the defined $100\mu\epsilon/m$ surface is indicated, the results strongly support the general concept of normality, or equivalently, the potential nature of Ω .

Tests are continuing to determine flow potential surfaces (SCISR's) at high homologous temperature (~ 0.5) on the representative austenitic alloy type 316 stainless steel. Similar testing is planned on the class of nickel-based alloys using Hastelloy. The objective is a general understanding of the nature and behavior of SCISR's under virgin conditions and conditions subsequent to inelastic deformation (i.e., creep, plasticity, recovery, etc.). Such an understanding is prerequisite to a rational representation of multiaxial, viscoplastic behavior.

From the experimentalist's viewpoint, most difficulty in conducting these experiments results from the stringent requirements placed on the performance of the strain measurement system. In multiaxial experiments of this type attempts are made to investigate inelastic response while maintaining the material in an unchanged state. This conflicting requirement can be approximated in probing type experiments in which very small changes in inelastic stain or inelastic strain rate are used as measures of inelastic response. Clearly, strain measurements systems used for this work must be capable of detecting these small changes which in practice requires near-micro-strain resolution. Another key requirement is that the output of the instrumentation should be linear over the entire measurement range of interest and also when loading passes through zero. This is because departure from linear behavior is used in effect as a measure of inelastic materials response. Nonlinearities resulting from the strain measurement system itself render such interpretations difficult or impossible to make. Perhaps the most limiting difficulty of all is that of crosstalk. One problem peculiar to biaxial and multiaxial experiments is that interaction or crosstalk can occur between the various forms of loading and straining. The possibility exists in tension-torsion experiments, for example, that loading in the axial sense can produce apparent torsional strains and vice versa. Clearly, crosstalk of this type precludes any meaningful investigation of normality.

In the present experiments, all of the difficulties described above were encountered to some degree. To obtain the necessary resolution, electronic gain of about $\times 100$ was used to set up the extensometer such that $\pm 3000\mu\epsilon \equiv \pm 10$ volts. Even though this value was relatively modest, "noise" problems were encountered with the amplifiers used for this purpose and the data generated in a number of probes was questionable as a result. Regarding linearity, post-test analysis of the data showed that the stress-time histories obtained in certain probes were nonlinear. This indicated that the integrators being used for test system control were drifting and providing less than adequate performance. Also, some difficulty was experienced with crosstalk. This was because no attempt was made to computer correct the strain signals in these preliminary experiments. The net result of these difficulties is that the directions of the strain rate vectors shown in figure 3 are somewhat open to

question. Also, the seemingly well behaved data obtained in Probe (14), figures 4 and 5, was duplicated in only eight of the remaining probes. This meant that limited data were available to construct the family of SCISR's shown in figure 6.

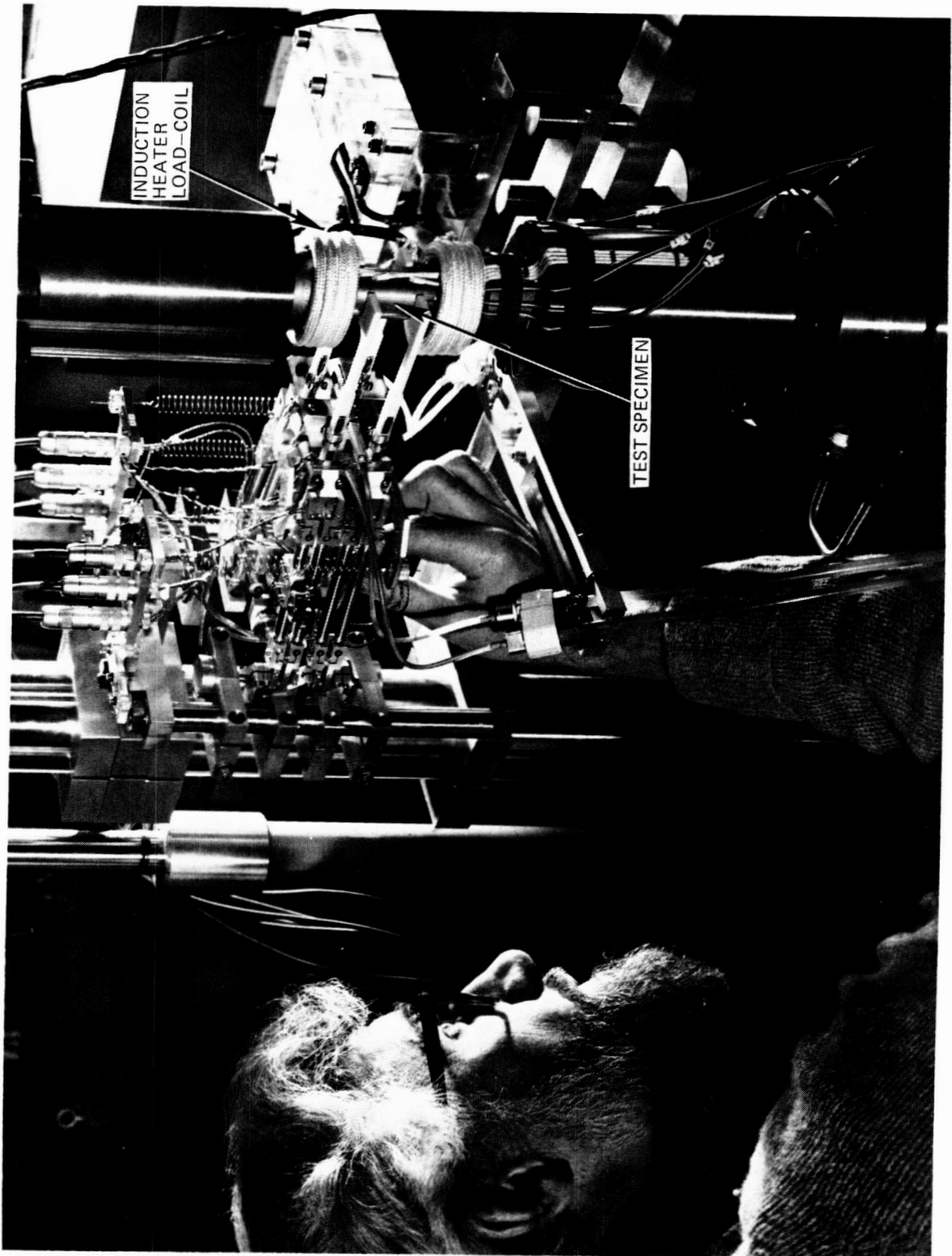
As the success of these experiments was seen to hinge on reliable biaxial strain measurement, an effort was initiated within the HOST program to resolve the difficulties noted above. In the case of the instrument used in the present experiments, the inductive transducers used for axial and torsional measurements are being replaced by capacitive type. The aim here is to eliminate "noise" problems in tests conducted at high homologous temperatures. It is also planned to investigate the feasibility of using a biaxial extensometer produced by MTS for the subject type of testing. Further, a third type of biaxial extensometer is being developed under contract at the Oak Ridge National Laboratory for possible use in high precision, probing type experiments.

REFERENCES

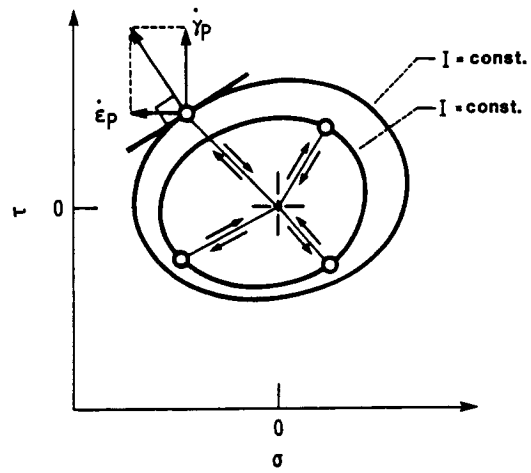
1. Bertsch, P. K. and Findley, W. N.: An Experimental Study of Subsequent Yield Surfaces - Corners, Normality, Bauschinger, and Related Effects. 4th U. S. National Congress of Applied Mechanics, 1962, pp. 893-907.
2. Philips, A.: The Foundations of Thermoplasticity-Experiment and Theory. Topics in Applied Continuum Mechanics, J. L. Zeman and F. Ziegler (eds.), Springer-Verlag, Wien-New York (1974).
3. Liu, D. C. and Greenstreet, W. L.: Experimental Studies to Examine Elastic-Plastic Behavior of Metal Alloys Used in Nuclear Structures. Constitutive Equations in Viscoplasticity Computational and Engineering Aspects, ASME Publication AMD-Vol. 20, Dec. 1976, pp. 35-56.
4. Ellis, J. R.; Robinson, D. N.; and Pugh, C. E.: Behavior of Annealed Type 316 Stainless Steel Under Monotonic and Cyclic Loading at Room Temperature. J. Nucl. Eng., and Design 47, 1978, pp. 115-123.
5. Ohashi, Y. and Tanaka, E.: Plastic Deformation Behavior of Mild Steel Along Orthogonal Trilinear Strain Trajectories in Three Dimensional Vector Space of Strain Deviator. J. Eng. Mat. Tech. 103(3), October 1981, pp. 187-292.
6. Ellis, J. R.; Robinson, D. N.; and Pugh, C. E.: Time Dependence in Biaxial Yield at Room Temperature. J. Eng. Mat. and Tech., Vol. 105, October 1983, pp. 250-256.
7. Coleman, B. D. and Gurtin, M. E.: Thermodynamics with Internal State Variables. J. Chem. Phys., Vol. 47, 1967, pp. 597-613.
8. Kestin, J. and Rice, J. R.: A Critical Review of Thermo-dynamics (Stuart, E. B. et al., eds.), Mono Book Corp., Baltimore, 1970, p. 275.
9. Rice, J. R.: On the Structure of Stress-Strain Relations for Time-Dependent Plastic Deformations in Metals. J. Appl. Mech., vol. 37, no. 3, Sept. 1970, pp. 728-737.
10. Hill, R. and Rice, J. R.: Constitutive Analysis of Elastic-Plastic Crystals at Arbitrary Strain. J. Mech. Phys. Solids, vol. 20, 1972, pp. 401-413.

11. Rice, J. R.: Mechanics and Thermodynamics of Plasticity. Constitutive Equations in Plasticity, ed. A. Argon, MIT Press, 1975.
12. Ponter, A. R. S. and Leckie, F. A.: Constitutive Relationships for the Time Dependent Deformation of Metals. J. Eng. Mater. Technol., vol. 98, no. 1, 1976, pp. 47-51.
13. Ponter, A. R. S.: Convexity and Associated Continuum Properties of a Class of Constitutive Relationships: J. de Mecanique 15(4), 1976, pp. 527-542.
14. Robinson, D. N. and Swindeman, R. W.: Unified Creep-Plasticity Constitutive Equations for 2-1/4 CR-1 MO Steel at Elevated Temperature. ORNL/TM-8444, Oct. 1982.
15. Robinson, D. N. et al: Constitutive Equations for Describing High-Temperature Inelastic Behavior of Structural Alloys. Proc. of Specialists Meeting on High-Temperature Structural Design Technology of LMFBRs, IAEA Report IWGFR/11, April 1976, pp. 44-57.
16. Robinson, D. N.: Constitutive Relationships for Anisotropic High-Temperature Alloys. J. Nucl. Eng. and Des., 83, 1984, pp. 389-396.
17. Chaboche, J. L.: On the Constitutive Equations of Materials Under Monotonic or Cyclic Loadings. Rech. Aerosp., 1983, pp. 31-43.
18. Brown, G. M.: Inelastic Deformation of an Aluminum Alloy Under Combined Stress at Elevated Temperature. J. Mech. Phys. Solids 18, 1970, pp. 383-396.
19. Robinson, D. N.: On the Concept of a Flow Potential and the Stress-Strain Relations of Reactor Systems Metals. ORNL/TM 5571, 1976.
20. Oytana, C.; Delobelle, P.; and Mermet, A.: Constitutive Equations Study in Biaxial Stress Experiments. J. Eng. Materials and Tech., vol. 104, 1982, pp. 1-11.
21. Robinson, D. N.: On Thermomechanical Testing in Support of Constitutive Equation Development for High-Temperature Alloys. NASA CR 174879, May 1985.
22. Robinson, D. N. and Ellis, J. R.: High Temperature Constitutive Modeling. Turbine Hot Section Technology 1984: Proceedings of a Conference Sponsored by NASA/Lewis Research Center, NASA Conference Publication 2339, Oct. 1984.
23. Ellis, J. R. and Robinson, D. N.: Some Advances in Experimentation Supporting Development of Viscoplastic Constitutive Models. NASA CR 174855, April 1985

ORIGINAL PAGE IS
OF POOR QUALITY



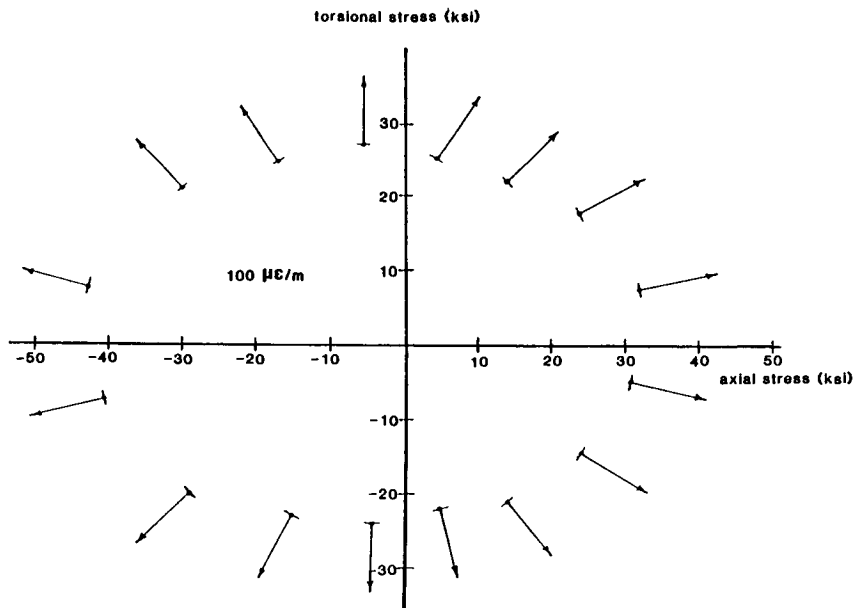
1. Experimental Setup Used in Determining Surfaces of Constant Inelastic Strain Rate (SCISRs).



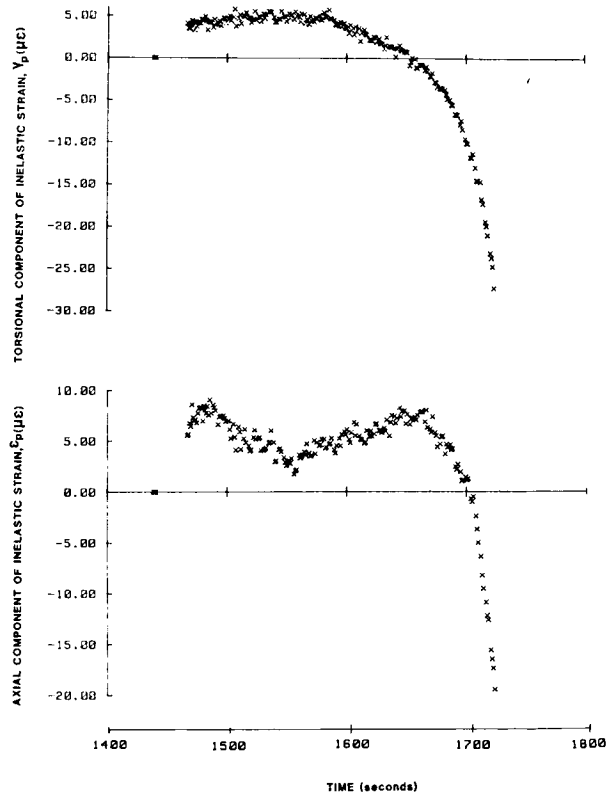
$$\begin{bmatrix} \dot{\epsilon}_p \\ \dot{\gamma}_p \end{bmatrix} = \begin{bmatrix} \dot{\epsilon} \\ \dot{\gamma} \end{bmatrix} - \begin{bmatrix} \dot{\sigma}/E \\ \dot{\tau}/G \end{bmatrix}$$

Computed
Measured
Controlled

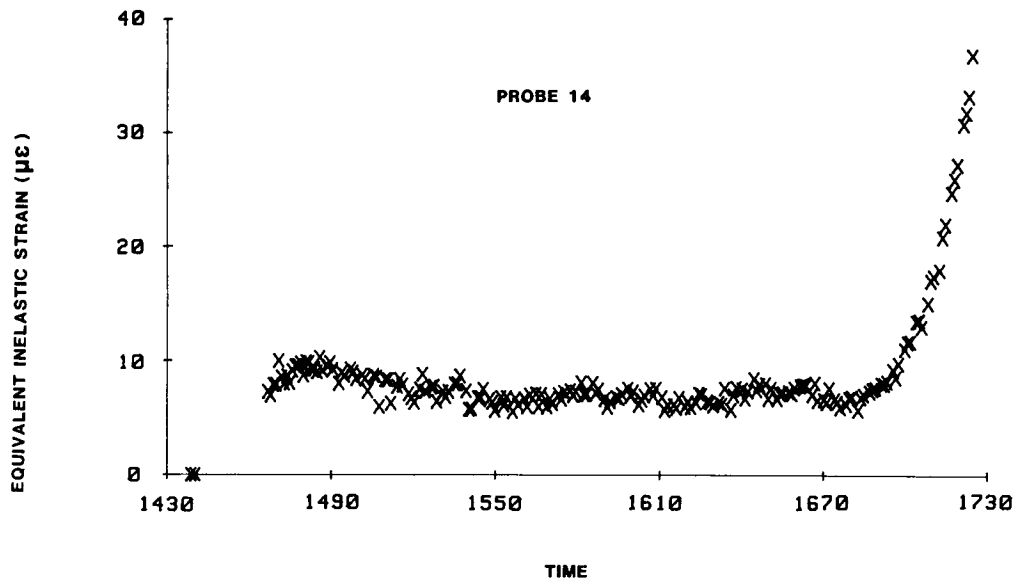
2. Approach Adopted in Determining SCISRs in Tension-Torsion Stress Space.



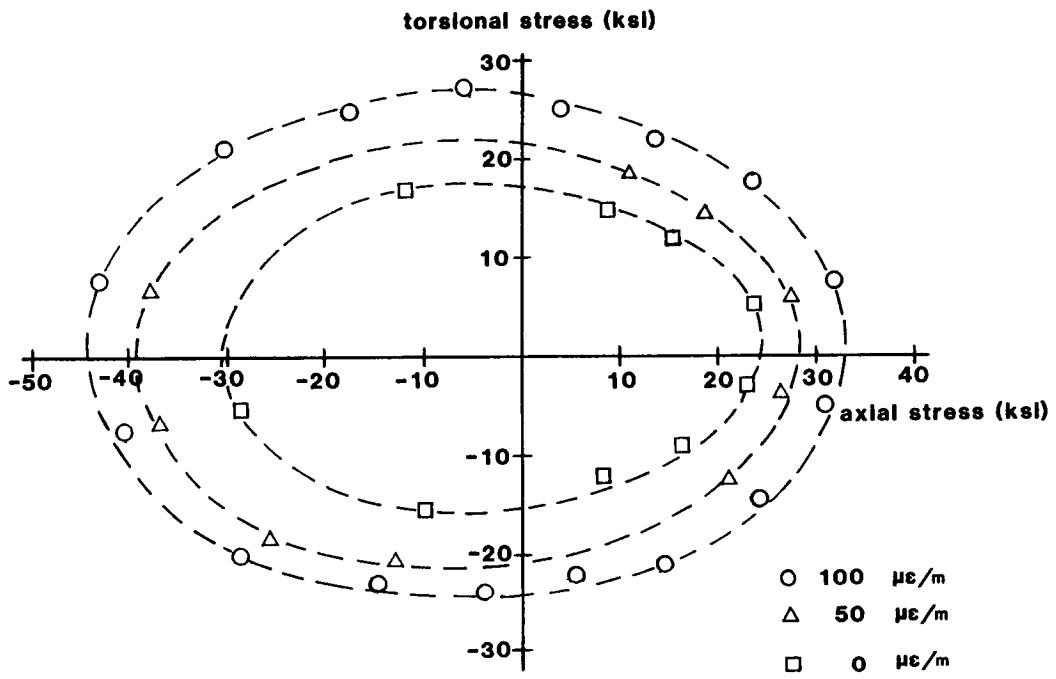
3. SCISR and Direction of the Inelastic Strain Rate Vectors: Target Value of Inelastic Strain rate = 100 $\mu\epsilon/m$.



4. Variation of the Axial and Torsional Components of Inelastic Strain During Probe (14).



5. Variation of Equivalent Inelastic Strain with Time During Probe (14).



6. SCISRs for Inelastic Strain Rates Ranging from Threshold to 100 $\mu\epsilon/m$.